(MS Submitted to JHM)

Size distributions and exposure concentrations of nanoparticles associated with the emissions of oil mists from fastener manufacturing processes

Ying-Fang Wang[a], Perng-Jy Tsai[a,b]*, Chun-Wan Chen[c], Da-Ren Chen, Yu-Tung Dai

[a]*Department of Environmental and Occupational Health, Medical College, National Cheng Kung University, 138, Sheng-Li Road, Tainan 70428, Taiwan*

[b]*Sustainable Environment Research Center, National Cheng Kung University, 1, University Road, Tainan 70101, Taiwan*

[c]*Institute of Occupational Safety and Health, Council of Labor Affairs, 99, Ln. 407, Hengke Road, Xizhi City, Taipei County 22143, Taiwan*

[d]*Department of Occupational Safety and Health, Chang Jung Christian University, 396, Sec. 1, Changrong Road, Guiren Dist., Tainan 71101, Taiwan*

***Correspondence author: P.-J. Tsai,** Tel.: +886-6-2353535 ext. 5806; Fax: +886-6-2752484; E-mail address: pjtsai@mail.ncku.edu.tw

Abstract

The aims of the present study were set out to measure size distributions and exposure concentrations of oil mist nanoparticles in three selected workplaces of the forming, threading, and heat treating areas in a fastener manufacturing plant by using a modified electrical aerosol detector (MEAD). The results were further compared with those simultaneously obtained from a nanoparticle surface area monitor (NSAM) and a scanning mobility particle sizer (SMPS) for the validation purpose. Results show that oil mist nanoparticles in the three selected process areas were formed mainly by the evaporation and condensation process. The measured size distributions of nanoparticles were consistently in the form of uni-modal. The fraction of nanoparticles deposited on the alveolar (AV) region was consistently much higher than that on the head airway (HD) and tracheobronchial (TB) regions in both number and surface area concentrations. However, a significant difference was found in the fraction of nanoparticles deposited on each individual region while different exposure metrics were used. Comparable results were found between results obtained from both NSAM and MEAD. After normalization, no significant difference can be found between the results obtained from SMPS and MEAD. It is concluded that the obtained MEAD results are suitable for assessing oil mist nanoparticle exposures.

Keywords: nanoparticle, exposure assessment, lung deposition, modified electrical aerosol detector, oil mist

1. Introduction

The manufacture of fasteners involves seven industrial processes, including the wiredrawing, forming, threading, cleaning, heat treatment, surface treatment, and packaging and shipping. Among them, the mineral oil-based metalworking fluids (MWFs) are used in the three processes of the forming, threading, and heat treatment, and thus might result in the emissions of oil mists to the workplace atmosphere and cause workers' exposures [1,2]. Epidemiological and animal studies have indicated that oil mist exposures might result in the laryngeal cancer, asthma, bronchial hyper-responsiveness, lipoid pneumonia, and lung cancer [3-6].

In principle, machining operations would mainly generate aerosols with particle sizes greater than 1 μm. However, the emissions of sub-micron and nano-sized particles could still be possible [7–10]. William et al. have reported that aerosols generated from an engine machining and assembly facility fell to the range from 0.023 μm to 0.1 μm [11]. In particular, for those involve 'hot' processes, such as welding, heat treatment, and high-speed machining processes, are known to generate nanoparticles [1,12–14]. It is known that MWFs are semi-volatile in nature, nanoparticles could be formed through the evaporation and condensation mechanisms after MWFs being "heated" during machining operations [15–16]. However, it should be noted that very few studies have been conducted to address workers' exposures to nanoparticles arising from oil mist emissions in workplaces which involved with the use of MWFs.

Nanoparticles are known for particles with diameters less than 0.1 μm (or 100 nm) [17]. Nanoparticles might cause serious inflammation in the deep lung because of their large particle numbers and surface areas [18–20]. Recent toxicological studies have suggested that they can easily penetrate cells or tissue and result in many

irreversible pulmonary health effects [21–23]. It has also been found that nanoparticles can penetrate to the brain via nasal mucosa and olfactory buds [23]. It is known that both the total surface area and total number concentrations are better exposure metrics for assessing ill-health effects caused by nanoparticle exposures than the metric of the total mass concentration [24–28]. In addition, ill-health effects associated with nanoparticle exposures are also affected by their deposition regions in the respiratory tract. Therefore, simultaneously measuring both the total surface area and total number concentrations of nanoparticles exposed to different regions of the respiratory tract is considered a better approach for characterizing nanoparticle exposures.

Many instruments, such as the condensation particle counter (CPC; Model 3020, TSI Inc., Shoreview, MN, USA), scanning mobility particle sizer (SMPS; Model 3934, TSI Inc., Shoreview, MN, USA), electrical low-pressure impactor (ELPI; Dekati Ltd., Tampere, Finland), and nano-micro-orifice uniform deposit impactor (Nano-MOUDI; Model 110, MSP Corp., Shoreview, MN, USA), have been used for assessing nanoparticle exposures for workers in various industries. However, the aforementioned devices can neither be used to directly measure their surface area concentrations, nor to estimate exposure concentrations in different regions of the respiratory tract (including the head airway (HD), tracheobronchial (TB) and alveolar (AV) regions). Recently, a nanoparticle surface area monitor (NSAM; Model 3550, TSI Inc., Shoreview, MN, USA) has been developed, based on the particle charging characteristics of an electrical aerosol detector (EAD; Model 3070a, TSI Inc., Shoreview, MN, USA) to directly measure surface area concentrations of nanoparticles deposited on both TB and AV regions of the respiratory tract [29– 30]. However, it should be noted that the above instrument can neither simultaneously

measure the surface area concentration of the HD region, nor the number concentrations of the HD, TB, and AV regions. More recently, a modified EAD (MEAD) has been developed by our research group to overcome the above mentioned shortcomings [31−32], and the device had been successfully used in the carbon black manufacturing workplaces [33].

The purposes of the present study were set out to use the MEAD to characterize size distributions of oil mist nanoparticles and their exposure concentrations to different regions of the respiratory tract, in both total surface and number concentrations, for workers in fastener manufacturing industry workplaces. The above results were further compared with those simultaneously obtained from SMPS and NSAM for the validation purpose.

2. Material and methods

2.1. Sampling sites

Field sampling were conducted at the three manufacturing processes of the forming, threading, and heat treatment associated with the use of MWFs. For the former two processes, the involvement of both the impaction and compression would lead to the increase in wire temperatures. Therefore, MWFs are used for the purpose of reducing wire temperature and extending machine life. After the threading process, the treaded products are quenched by passing through MWFs. Then, the products are annealed to room temperature. Finally, they are tempered by raising temperatures from 650°C to 1,500°C to obtain products with requested hardness and toughness [34].

In the present study, an outdoor sampling site, located at the outside of office building of the selected fastener manufacturing plant, was also selected to determine the background concentration of measured nanoparticles.

2.2. Sampling instruments

A MEAD was used to conduct samplings for nanopartilces in the present study. The MEAD was installed with a high voltage power supply (Stanford Research Systems Inc., Model PS325/2500V–25W, Sunnyvale, CA, USA) to have its voltages of the ion trap become variable (range: 20V–2500V). During samplings, the readings of the electrometer were recorded respectively while the voltages of the ion trap were consecutively set at 20V, 100V, 200V, 500V, 1000V, 1500V, 2000V, and 2500V (each for ten seconds) for each run [31]. Two reference instruments were simultaneously used to measure nanoparticles in order to validate results obtained from the MEAD. The first one was the NSAM (TSI Inc., Model 3550, St. Paul, MN, USA) which was used to measure surface area concentrations of nanoparticles deposited on both TB and AV regions of the respiratory tract [30]. The second one was the SMPS (TSI Inc., Model 3936, St. Paul, MN, USA) which was used to measure the number concentrations of nanoparticles of different particle sizes.

2.3. Sampling methods

For all selected workplaces (including the forming, threading, heat treatment processes, and outdoor sampling site), samplings were conducted for continuous four days. On each sampling day for each selected workplace, one MEAD, one NSAM and one SMPS were placed side-by-side at the location nearest to worker's breathing zone (i.e., location ~1.5 m above the ground level). Samplings were conducted from 08:00 AM to 10:00 AM and from 08:00 AM to 12:00 AM to determine the outdoor atmospheric background concentration and workers' daily exposure concentrations, respectively. Considering workers in these three selected areas worked for 24 h per day (three-shift), no workplace background concentrations could be measured.

2.4. Data analyses

In the present study, a data-reduction scheme was used to retrieve the size

140 distribution of sampled nanoparticles based on readings obtained the eight preset
141 voltages of the MEAD. Detailed computation processes can be seen in our previous
142 publication [31]. The resultant size distributions were used to predict depositions of
143 nanoparticles at the H, TB, and AV regions of the respiratory tract using the UK
144 National Radiological Protection Board's (NRPB's) LUDEP Software [35]. The
145 above software was established based on ICRP 66 lung deposition models [36]. In the
146 present study, we assumed the breathing pattern of workers can be described as
147 follows:

148 –Breathing type: nose only

149 –Functional lung residual capacity: 3301 mL

150 –Breathing rate: 20 Breath/min

151 –Ventilation rate: 1.5 m^3/h

152 –Activity level: light exercise.

153 The above criteria were the same as that prescribed for NSAM [30]. Fig. 1. shows
154 three predicted deposition curves of the HD, TB, and AV regions based on the above
155 assumptions, respectively. Here, it should be noted that the above predicted deposition
156 curves are only suitable for workers with light exercise conditions under nose-only
157 breathing conditions. The above working scenarios were quite comparable to those
158 workers in the three selected processes via our field observations.

159 **3. Results and discussion**

160 **3.1. Size distributions of nanoparticles**

161 Table 1 shows size distributions of nanoparticles (measured particle size range:
162 1–1000 nm) in the atmosphere of the three selected workplaces and the outdoor
163 ambient air. It can be seen that the count median diameter (CMD) and the
164 corresponding geometric standard deviation (σ_g) for nanoparticles of the outdoor

ambient air were 41.1 nm and 2.2, respectively. The above results were similar to the results obtained from Heitbrink et al. and Wake [11, 37]. As shown in Fig. 2., size distributions of nanoparticles were consistently in the form of the uni-modal for samples collected from the forming area, threading area, and heat treating area with CMD and its corresponding σg as 26.9 nm and 2.64, 23.2 nm and 2.86, and 22.5 nm and 2.98, respectively. In an engine machining and assembly facility workplace atmosphere, Heitbrink et al. found that the resultant uni-modal nanoparticles could be mainly contributed by the evaporation/condensation because of MWFs being heated at the interface between the tools and the components during machine operations [11]. At this stage, it might not be possible to explain the intrinsic differences in CMD among three studied industrial processes because factors associated with the evolution of aerosols in the field were very complicated (such as saturated vapor pressure, surface tension, and molecular weights of the involved MWFs, etc.) [38–39]. However, our results are quite comparable to those conducted by Heitbrink et al. (i.e., particle size range= 20–40 nm) [11].

3.2. Number concentrations and surface area concentrations of nanoparticles

Table 2 shows the number and surface area concentrations of nanoparticles (measured particle size range: 1–1000 nm) for the outdoor atmospheric background and the three selected workplaces. The mean number concentrations for the forming area, threading area, and heat treating area (=1.42–3.47×10^5 #/cm^3) were significantly higher than that of the outdoor environment (=0.126×10^5 #/cm^3) (p<0.05). The above results clearly indicate that process emissions could effectively elevate the number concentrations of nanoparticles in workplace atmospheres. However, we also found that their workplace concentrations fell within the range obtained from an engine machining and assembly plant conducted by Heitbrink et al. (= 0.29–4.4×10^5 #/cm^3)

190 [11].

191 The mean number concentrations obtained from the forming area (=2.13×10^5
192 #/cm^3) was significantly higher than the threading area (=1.42×10^5 #/cm^3)
193 (nonparameteric Mann-Whitney test, $p<0.05$). Based on our previous study [38], the
194 measured surface temperatures on the molder of the forming machine (=75.8± 19.8℃)
195 were higher than that on the surface of the threading gear (=69.6± 17.1℃). In
196 addition, we also found that the workplace area of the threading process (=734.4 m^2)
197 was much larger than that of forming process (=194.7 m^2). Therefore, it could be
198 expected that the forming area had higher number concentrations than that of the
199 threading area by considering the generation of oil mists due to the evaporation and
200 condensation processes, and the dilution effect associated the volumes of the above
201 two workplaces. Finally, we found the heat treating area had the highest number
202 concentration among the three selected industrial processes ($p<0.005$). In the present
203 study, the temperatures measured from those MWFs tanks used in quenching and
204 tempering steps of heat treating operations (850–1300℃ and 650–1300℃,
205 respectively) were much higher than the temperatures measured from the other two
206 processes (as described above). Indeed, both temperatures of fluid and air would
207 affect how semi-volatile substances evaporate and condensate in the workplace
208 atmosphere [40–41]. Since the workplace temperatures of the heat treating process
209 were still less than 30℃, the highest number concentration found in the heat treating
210 process would be theoretically plausible.

211 Finally, the trends found in the measured number concentrations (as described
212 above) can also be seen in their corresponding surface area concentrations. In the
213 present study, significant differences can be found between the mean surface area
214 concentration of the outdoor atmospheric background (=0.218×10^3 $\mu m^2/cm^3$) and that

of the concentrations of the three selected areas (=1.11–7.48×10^3 μm^2/cm^3) (p <0.05). Moreover, workplace concentrations of the threading area (=2.03×10^3 μm^2/cm^3) and the forming area (=3.06×10^3 μm^2/cm^3) were lower than that of the heat treating area (=5.39×10^3 μm^2/cm^3).

Furthermore, we compared the estimated number concentrations of the three workplaces obtained from MEAD with that obtained from SMPS. Significant differences can be found between measured values (paired t-test, p<0.05) obtained from MEAD and that from SMPS. In particular, values obtained from the MEAD were consistently higher than that from SMPS. Considering measuring principles of the MEAD was different from that of SMPS, the existence of systemic differences between their measured results could be theoretically plausible. A similar result can also be found in a study conducted by Woo et al. in measuring atmospheric nanoparticle concentrations [42]. In this study, the results obtained from the SMPS were used as the reference to normalize the values obtained from the MEAD. No significant difference can be found between the measured values obtained from SMPS and the corresponding normalized MEAD values (paired t-test, p>0.05) (Fig. 3.). The relationship between the results obtained from SMPS (i.e., x) and the normalized MEAD results (i.e., y) was found as y=0.93 x (n=18, corrected-R^2=0.74). Therefore, the number concentrations obtained from MEAD were further validated.

3.3. Estimated concentrations of nanoparticles deposited on different regions of the respiratory tract

In this study, the measured size distribution data was further used to estimate both the number and surface area concentrations of nanoparticles deposited on different regions of the respiratory tract for the three selected workplaces. Table 3 shows the estimated number concentrations (and their fractions) deposited on the three regions

of the HD, TB, and AV of the respiratory tract. For the forming area, the estimated number concentrations for the HD, TB, and AV regions were 0.252×10^5 #/cm^3, 0.275×10^5 #/cm^3, and 0.861×10^5 #/cm^3, respectively. For the threading area were 0.191×10^5 #/cm^3, 0.204×10^5 #/cm^3, and 0.536×10^5 #/cm^3, respectively. For the heat treating area were 0.515×10^5 #/cm^3, 0.517×10^5 #/cm^3, and 1.27×10^5 #/cm^3, respectively. The fractions of nanoparticles deposited on the three regions, while presented in sequence, were (1) forming area: AV (62%) > TB (20%) >HD (18%), (2) threading area: AV (57%)> TB (22%) > HD (21%), and (3) heat treating area: AV (56%) >TB (22%) and HD (22%). The above results clearly indicate that the fractions of nanoparticles deposited on the AV region were much higher than that of the other two regions for all selected workplaces.

Table 4 shows the estimated surface area concentrations (and their fractions) deposited on the three regions of the HD, TB, and AV of the respiratory tract for the three selected workplaces. For the forming area, the estimated surface area concentrations for the HD, TB, and AV regions were 2.73×10^2 μm^2/cm^3, 1.64×10^2μm^2/cm^3, and 6.71×10^2μm^2/cm^3, respectively. For the threading area, they were 1.37×10^2μm^2/cm^3, 0.705×10^2μm^2/cm^3, and 2.89×10^2μm^2/cm^3, respectively. For the heat treating area, they were 3.91×10^2μm^2/cm^3, 1.77×10^2μm^2/cm^3, and 7.34×10^2μm^2/cm^3, respectively. The fractions of nanoparticles deposited on the three regions, while presented in sequence, shared the same trend as (1) forming area: AV (60%) >HD (25%) >TB(15%), (2) threading area: AV (58%) >HD (28%) > TB (14%), and (3) heat treating area: AV (56%) >HD (30%) >TB (14%). By comparing the results shown in Table 3 and Table 4, significant differences can be found in the fractions of nanoparticles deposited on each individual region while different exposure metrics were adopted. Our results clearly indicate the importance for

265 simultaneously measuring both the surface area and number concentrations of
266 nanoparticles deposited on different regions of the respiratory tract for nanoparticle
267 exposure assessments.

268 Fig. 4. compares the results of the surface area concentrations deposited on both
269 the TB and AV regions obtained from MEAD with that obtained from NSAM. For the
270 concentrations estimated for the TB region, the results obtained from the NSAM for
271 the forming area, threading area, and heat treating area were 1.19×10^2 $\mu m^2/cm^3$,
272 0.562×10^2 $\mu m^2/cm^3$, and 1.27×10^2 $\mu m^2/cm^3$, respectively. The above results were
273 quite comparable to those obtained from MEAD (= 1.64×10^2 $\mu m^2/cm^3$, 0.705×10^2
274 $\mu m^2/cm^3$, and 1.77×10^2 $\mu m^2/cm^3$, respectively) (t-test, $p>0.05$). The same trend can
275 also be found for the concentrations estimated for the AV region (NSAM= 6.73×10^2
276 $\mu m^2/cm^3$, 2.65×10^2 $\mu m^2/cm^3$, and 5.30×10^2 $\mu m^2/cm^3$, respectively; and
277 MEAD=6.71×10^2 $\mu m^2/cm^3$, 2.89×10^2 $\mu m^2/cm^3$, and 7.34×10^2 $\mu m^2/cm^3$, respectively)
278 (t-test, $p>0.05$). Considering both NSAM and MEAD sharing the same measuring
279 principles (i.e., particle charging efficiency and particle electrical mobility),
280 comparable results obtained from both instruments could be theoretically expectable.

281 **4. Conclusions**

282 We found that size distributions of nanoparticles were consistently in the form of
283 uni-modal for the three selected process areas. It could be mainly contributed by the
284 evaporation and condensation processes of MWFs. For both number and surface area
285 concentrations, the fractions of nanoparticles deposited on the AV region were much
286 higher than that of the other two regions of the TB and HD for all selected workplaces.
287 However, a significant difference was found in the fractions of nanoparticles
288 deposited on each individual region of the respiratory tract while different exposure
289 metrics were adopted. Our results clearly indicate the importance for simultaneously

measuring both the surface area and number concentrations of nanoparticles deposited on different regions of the respiratory tract for nanoparticle exposure assessments. In the present study, results obtained from both NSAM and MEAD were quite comparable. In addition, no significant difference can be found between the measured values obtained from SMPS and the corresponding MEAD values after being normalized. The above results clearly indicate that the measured MEAD results would be theoretically plaussible.

ACKNOWLEDGEMENT

We are grateful to the Institute of Occupational Safety and Health (IOSH) in Taiwan for funding this research project.

REFERENCES

[1] D. L. Thornburg, Mist genetration during metal machining. J. Trib. 122 (2000) 544–549.

[2] D. J. Michalek, W. W. S. Hii, J. S. Sun, K. L. Gunter, Experimental and analytical efforts to characterize cutting fluid mist formation and behavior in machining. Appl. Occup. Environ. Hyg. 18 (2003) 842–854.

[3] M. Russi, R. Dubrow, J. T. Flannery, M. R. Cullen, S. T. Mayne, Occupational exposure to machining fluids and laryngeal cancer risk: contrasting results using two separate control groups. Am. J. Ind. Med. 31 (1997) 166–171.

[4] A. E. Ellen, J. S. Thomas, K. David, R. W. Susan, J. M. Douglas, M. K. Susan, S. Stuart, R. M. Richard, Respiratory health of automobile workers and exposures to metal-working fluid aerosols: lung spirometry. Am. J. Ind. Med. 39 (2001) 443–453.

[5] S. M. Kennedy, Y. M. Chan, K. Teschke, B. Karlen, Change in airway responsiveness among apprentices exposed to metalworking fluids. Am. J. Respir. Crit. Care Med. 159 (1999) 87–93.

[6] N. Kazerouni, T. L. Thomas, S. A. Petralia, R. B. Hayes, Mortality among workers exposed to cutting oil mist: update of previous reports. Am. J. Ind. Med. 38 (2000) 410–416.

[7] T. L. Chan, J. B. D'Arcy, J. Siak, Size characteristics of machining fluid aerosols in an industrial metalworking environment. Appl. Occup. Environ. Hyg. 5 (1990) 162–170.

[8] J. Dash, J. B. D'Arcy, A. Gundrum, J. Sutherland, J. Johnson, D. Carlson, Characterization of fine particles from machining in automotive plants. J. Occup. Environ. Hyg. 2 (2005) 609–625.

[9] W. A. Heitbrink, J. B. D'Arcy, J.M. Yacher, Mist genetration at a machining center. Am. Ind. Hyg. Assoc. J. 61 (2000) 22–30.

[10] W. A. Heitbrink, J. M. Yacher, G. J. Deye, A. B. Spencer, Mist control at machining center, Part 1: mist characterization. Am. Ind. Hyg. Assoc. J. 61 (2000) 275–281.

[11] W. A. Heitbrink, D. E. Evans, T. M. Peters, T. J. Slavin, Characterization and mapping of very fine particles in an engine machining and assembly facility. J. Occup. Environ. Hyg. 4 (2007) 341–351.

[12] J. Vincent, C. Clement, Ultrafine particles in workplace atmospheres. The Royal Society. 358 (2000) 2673–2682.

[13] A. S. Ross, K. Teschke, M. Brauer, S. M. Kennedy, Determinants of exposure to metalworking fluid aerosol in small machine shops. Ann. Occup. Hyg. 48 (2004) 383–391.

[14] J. R. Portela, J. Lopez, E. Nebot, Martínez de la Ossa E, Elimination of cutting oil wastes by promoted hydrothermal oxidation. J. Hazared Mater. 88 (2001) 95–106.

[15] J. Thornburg, D. Leith, Size distribution of mist genetrated during metal machining. Appl. Occup. Environ. Hyg. 15 (2000) 618–628.

[16] J. F. Pankow, An absorption model of the gas/particle partitioning of organic compounds in the atmosphere. Atmos. Environ. 28 (1994) 185–188.

[17] A. Peters, H. E. Wichmann, T. Tuch, J. Heinrich, J. Heyder, Respiratory effects are associated with the number of ultrafine particles. Am. J. Respir. Crit. Care Med. 155 (1997) 1376–1383.

[18] W. G. Kreyling, M. Semmler, F. Erbe, P. Mayer, S. Takenaka, H. Schulz, Translocation of ultrafine insoluble iridium particles from lung epithelium to extrapulmonary organs is size dependent but very low. J. Toxicol. Environ. Health. 65 (2002) 1513–1530.

[19] G. Oberdörster, Pulmonary effects of inhaled ultrafine particles. Int. Arch. Occup. Environ. Health. 74 (2001) 1–8.

[20] K. Donaldson, D. Brown, A. Clouter, R. Duffin, W. MacNee, L. Renwick, L. Tran, V. Stone, The pulmonary toxicology of ultrafine particles. J. Aerosol. Med. 15 (2002) 213–220.

[21] D. W. Dockery, C. A. Pope, X. Xu, J. D. Spengler, J. H. Ware, M. E. Fay, An Association between air pollution and mortality in six U.S. cities. N. Engl. J. Med. 329 (1993) 1753–1759.

[22] G. Oberdörster, Toxicology of ultrafine particles: in vivo studies. Philos. Trans. R. Soc. Lond. A. 358 (2000) 2719–2740.

[23] E. Oberdörster, Manufactured nanomaterials (Fullerenes, C60) induce oxidative stress in the brain of juvenile largemouth bass. Environ. Health Perspect. 112 (2004) 1058–1062.

[24] G. Oberdörster, Significance of particle parameters in the evaluation of exposure-dose-response relationships of inhaled particles. Part. Sci. Technol. 14 (1996) 135–151.

[25] K. Donaldson, X. Y. Li, W. MacNee, Ultrafine (nanometer) particle mediated lung injury. J. Aerosol Sci. 29 (1998) 553–560.

[26] C. L. Tran, D. Buchanan, R. T. Cullen, A. Searl, A. D. Jones, K. Donaldson, Inhalation of poorly soluble particles. Ⅱ. Influence of particle surface area on inflammation and clearance. Inhal. Toxicol. 12 (2005) 1113–1126.

[27] A. Elder, R. Gelein, J. N. Finkelstein, K. E. Driscoll, J. Harkema, G. Oberdörster, Effects of subchronically inhaled carbon black in three species. Ⅰ. Retention kinetics, lung inflammation, and histopathology. Toxicol. Sci. 88 (2005) 614–629.

[28] T. Stoeger, C. Reinhard, S. Takenaka, A. Schroeppel, E. Karg, B. Ritter, J. Heyder, H. Schulz, Instillation of six different ultrafine carbon particles indicates a surface area threshold dose for acute lung inflammation in mice. Environ. Health Perspect. 114 (2006) 328–333.

[29] W. E. Wilson, H. S. Han, J. Stanek, J. Turner, D. R. Chen, D. Y. H. Pui, Use of the electrical aerosol detector as an indicator of the surface area of fine particles deposited in the lung. J. Air & Waste Manage. Assoc. 57 (2007) 211–220.

[30] H. Fissan, A. Trampe, S. Neunman, D. Y. H. Pui, W. G. Shin, Rationale and principle of an instrument measuring lung deposition area. Journal of Nanoparticle Research. 9 (2007) 53–59.

[31] L. Li, D. R. Chen, P. J. Tsai, Use of An Electrical Aerosol Detector (EAD) for Nanoparticle Size Distribution Measurement. Journal of Nanoparticle Research. 11 (2009a) 111–120.

[32] L. Li, D. R. Chen, P. J. Tsai, Evaluation of an Electrical Aerosol Detector (EAD) for the Aerosol Integral Parameter Measurement. J. Electro. 67 (2009b) 765–773.

[33] Y. F. Wang, P. J. Tsai, C. W. Chen, D. R. Chen, D. J. Hsu, Using a modified electrical aerosol detector (MEAD) to predict nanoparticle exposures to different regions of the respiratory tract for workers in a carbon black manufacturing industry. Environ. Sci. Tech. 44 (2010) 6767–6774.

[34] H. H. Daniel, D. S. Richard, Heat Treating Fasteners – Part 1: Tips of the Trade. Fastener Technology International. (2008) 34–37.

[35] A. C. James, M. R. Bailey, M. D. Dorrian, LUDEP Software, Version 2.07: program for implementing ICRP 66 Respiratory tract model. RPB, Chilton, Didcot, OXON. OX11 ORQ UK, 2000.

[36] ICRP, International Commission on Radiological Protection. Human respiratory tract model for radiological protection, Publication 66; Oxford, Pergamon: London, UK, 1994.

[37] D. Wake, Ultrafine particles in the workplace. HSL Report number ECO/00/18, 2001.

[38] M. R. Chen, P. J. Tsai, C. C. Chang, T. S. Shih, W. J. Lee, P. C. Liao, Particle size distributions of oil mists in workplace atmospheres and their exposure

concentrations to workers in a fastener manufacturing industry. J. Hazared Mater. 146 (2007) 393–398.

[39] W. C. Hinds, Condensation and evaporation, in: aerosol technology properties, behavior, and measurement of airborne particles. Second ed. John Wiely and Sons, Inc. New York, USA, 1999, pp. 278–303.

[40] S. Cooper, D. Leith, Evaporation of metalworking fluid mist in laboratory and industrial mist collectors. AIHA J. 59 (1998) 45–51.

[41] R. C. Raynor, S. Cooper, D. Leith, Evaporation of polydisperse multicomponent oil droplets. AIHA J. 57 (1996) 1128–1136.

[42] K. S. Woo, D. R. Chen, D. Y. H. Pui, W. E. Wilson, Use of continuous measurements of integral aerosol parameters to estimate particle surface area. Aerosol Sci. Tech. 34 (2001) 57–65.

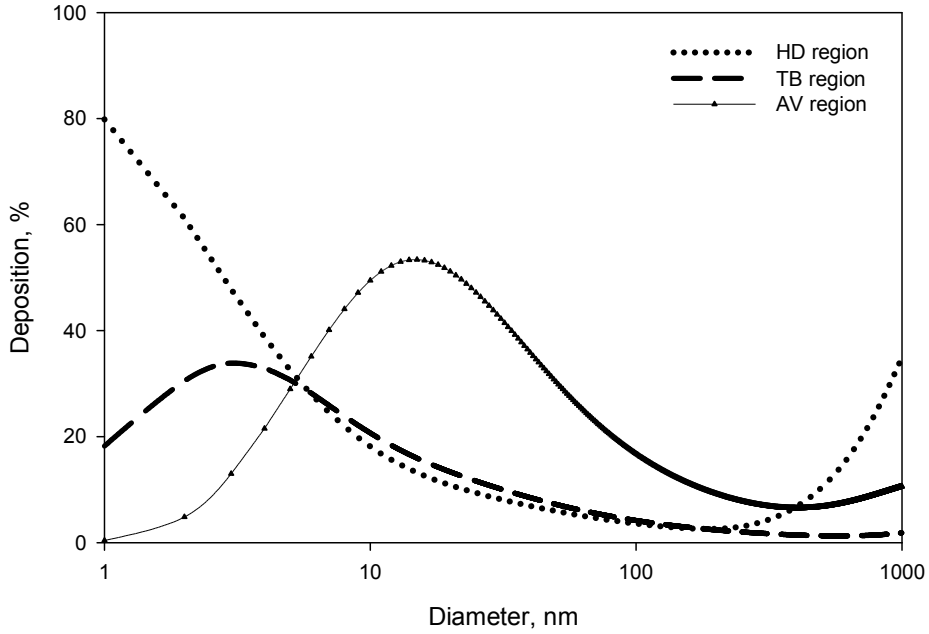

Fig. 1. Calculated particle deposition curves as a function of particle size for the Head Airway (HD), Tracheobronchial (TB), and Alveolar (AV) regions of a human lung (based on the model given in ICRP [36]).

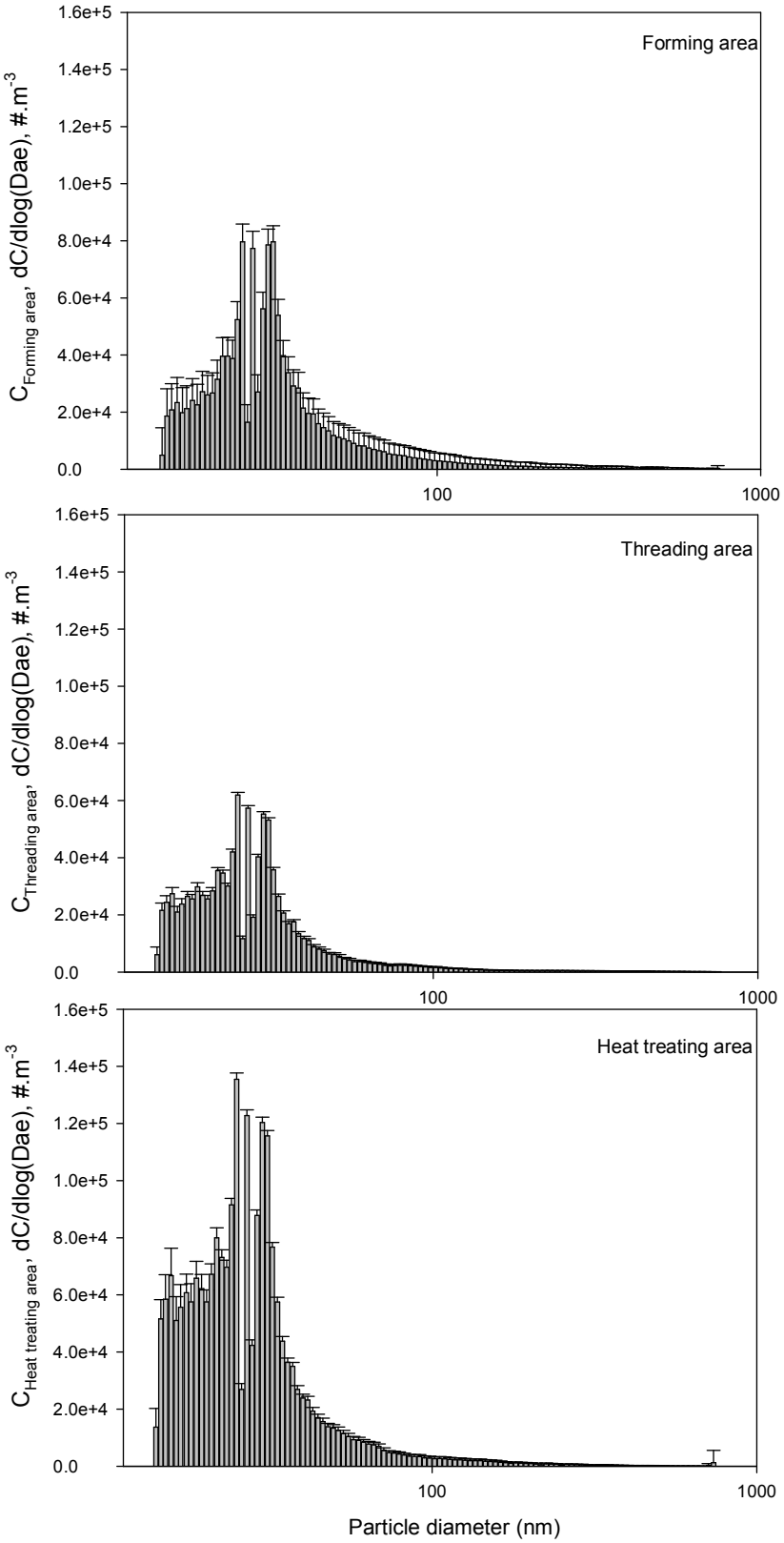

428

429 Fig. 2. Particle number-based size distributions in the three selected area were

430 measured by MEAD in activity.

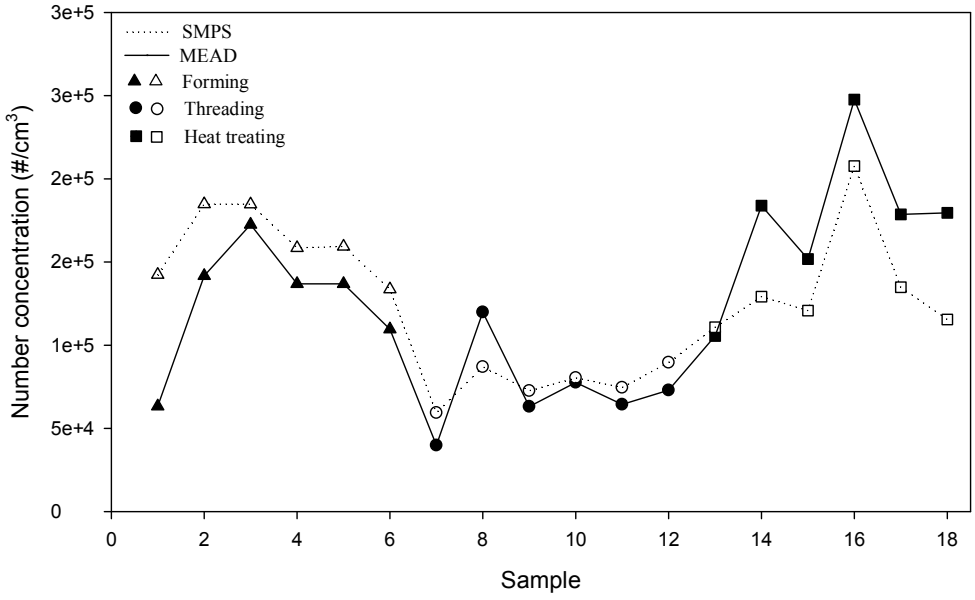

Fig. 3. Comparing number concentrations obtained from SMPS with that from MEAD after being normalized.

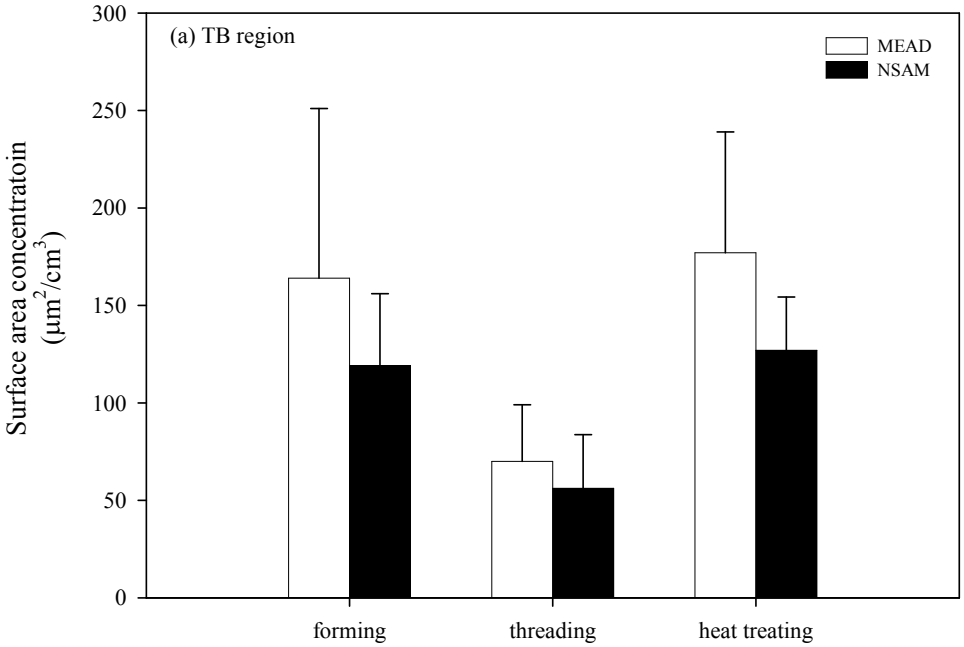

434

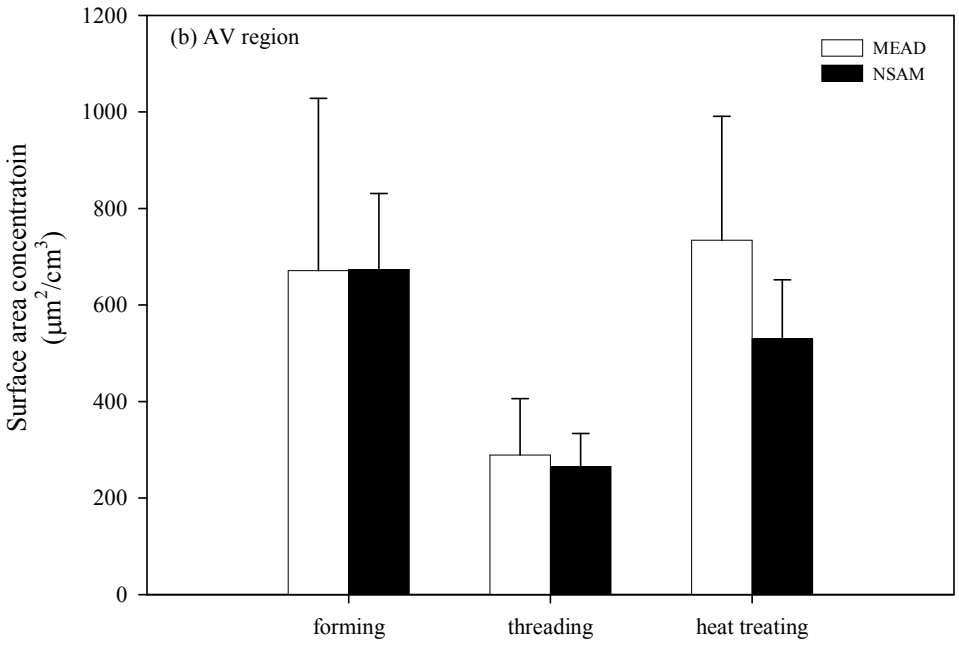

435

436 Fig. 4. Confirmations of nanoparticles deposited in (a) TB region and (b) AV region

437 were measured by the MEAD and NSAM.

438 Table 1 Number-based size distributions of nanoparticles (1–1000 nm) in the selected

439 workplace were measured by MEAD (n=6).

work area	Number-based size distribution (nm)	
	CMD(range)	σg
forming	26.9(25.3–30.1)	2.64
threading	23.2(21.1–25.2)	2.86
heat treating	22.5(20.3–25.2)	2.98
Ambient*	41.1	2.21

440 *: n=1
441

442

443 Table 2 Estimated total number concentrations (10^5 #/cm^3) and total surface area

444 concentrations (10^3 μm^2/cm^3) for nanoparticles (1–1000 nm) found in the selected

445 work area (n=6)

work area	Total number concentration (10^5 #/cm^3)		Total surface area concentration (10^3 μm^2/cm^3)	
	mean±SD	range	mean±SD	range
forming	2.13±1.05	1.23–3.35	3.06±1.14	1.77–4.82
threading	1.42±0.572	0.772–2.33	2.03±0.733	1.11–3.33
heat treating	3.47±1.22	2.05–4.80	5.39±1.46	3.18–7.48
Ambient*	0.126	–	0.218	–

446 *: n=1

447 Table 3 Estimated number concentrations (10^5 #/cm^3) deposited in the HD, TB, and

448 AV regions of the respiratory tract for nanoparticles (1–1000 nm) found in the

449 selected workplace (n=6)

work area	Total deposited conc.	HD		TB		AV	
		Conc.	Fraction (%)	Conc.	Fraction (%)	Conc.	Fraction (%)
forming	1.38±1.07	0.252±0.203	18	0.275±0.221	20	0.861±0.643	62
threading	0.922±0.372	0.191±0.083	21	0.204±0.082	22	0.536±0.212	57
heat treating	2.27±0.791	0.515±0.176	22	0.517±0.183	22	1.27±0.454	56

450

451

452 Table 4 Estimated surface area concentrations ($10^2 \mu m^2/cm^3$) deposited in the HD, TB,

453 and AV regions of the respiratory tract for nanoparticles (1–1000 nm) found in the

454 selected workplace (n=6)

work area	Total deposited conc.	HD		TB		AV	
		Conc.	Fraction (%)	Conc.	Fraction (%)	Conc.	Fraction (%)
forming	11.1±5.90	2.73±1.45	25	1.64±0.873	15	6.71±3.57	60
threading	4.97±2.01	1.37±0.551	28	0.705±0.298	14	2.89±1.17	58
heat treating	13.2±4.57	3.91±1.37	30	1.77±0.627	14	7.34±2.57	56

455